

Control of kinetic opinion dynamics in popularity-adaptive social networks

Giacomo Albi*

Elisa Calzola†

Matteo Piu‡

Abstract

This paper presents a mathematical model for opinion dynamics in popularity-adaptive social networks, where both opinion spreading and the evolution of social media contacts depend on agents' popularity and the prominence of their views. While previous approaches accounted for the influence of popularity on opinion dynamics, we introduce a novel feedback mechanism in which opinion affects the formation of contacts. Within a kinetic modeling framework, we describe the evolution of the coupled dynamics of opinions and network structure, incorporating a class of control laws in order to promote interactions with popular individuals and amplify dominant opinions. Such control strategies are introduced to influence both opinion formation and connectivity, representing interventions such as awareness campaigns or moderation policies. Numerical results show how control strategies can mitigate polarization, foster consensus, or guide opinion distributions in dynamically evolving networks.

1 Introduction

Kinetic theory has become a central mathematical framework for the description of large systems of interacting agents, providing tractable models capable of capturing the emergence of collective behaviours across a wide spectrum of applications, ranging from economics and traffic dynamics to the social and biological sciences [10, 34]. In these settings, Boltzmann-type equations allow to derive mesoscopic descriptions starting from simple interaction rules, thus linking microscopic decision processes to macroscopic observables. Applications of such paradigm span socio-economic models for price formation and wealth redistribution [14, 16, 18, 24, 35, 39], kinetic descriptions of population and epidemic dynamics [13, 15, 20], and applications in transportation engineering and crowd modelling [2, 6, 11, 19, 26, 29, 36].

Within this kinetic framework, opinion formation is a central example for interaction mechanisms, where repeated social exchanges give rise to dynamics well described by Boltzmann-type models, capturing consensus, polarisation and fragmentation as studied in [21, 22, 27, 28, 38]. Of particular importance is the extension of these modelling frameworks to account for an additional layer of complexity such as individual popularity, typically quantified by the number of connections or followers in a social networks. Hence, recent developments have focused on coupling opinion evolution with the dynamics of the underlying social connectivity structure, see for example [1, 5, 25, 37].

Here we focus on kinetic model for the evolution of joint density of opinions and contacts, where each agent is represented by an opinion $v \in [-1, 1]$ and a popularity variable $c \geq 0$ measuring its social connections. Following the approach proposed in [5, 9], we assume that dynamics of opinions depend on agents' popularity. Furthermore, we introduce a feedback mechanism in which agents' opinions influence the evolution of their social connections, while the strength of opinion interactions remains modulated by the individuals' relative popularity. This second assumption has not been considered in previous works within this context, nevertheless it is supported by empirical evidence showing that individuals tend to form or dissolve connections based on opinion similarity. This phenomenon is widely documented in studies on homophily, echo chambers, and opinion-driven rewiring in online social networks, see for instance [17, 30, 32, 33].

In this modelling framework, we also investigate the impact of control mechanisms acting on both the contact dynamics and the opinion evolution. Control strategies in opinion modelling have been explored at various scales see for example [3, 12, 23]. Here we follow the approach introduced in [7, 8], deriving two type of feedback controls, the first acting over the contact formation and designed to counteract the endogenous decay of contacts by mitigating unfavourable trends in the visibility of selected agents or groups. A second control term acts at the

*University of Verona, Department of Computer Science, Strada le Grazie 15, 37134 Verona (Italy). Email: giacomo.albi@univr.it

†University of Ferrara, Department of Mathematics and Computer Science, Via Nicolò Machiavelli 30, 44121 Ferrara (Italy). Email: elisa.calzola@unife.it

‡University of Verona, Department of Computer Science, Strada le Grazie 15, 37134 Verona (Italy). Email: matteo.piu@univr.it

opinion level, steering agents toward prescribed target positions whenever activation criteria based on connectivity or local opinion density are satisfied.

The integration of such kinetic framework with control thus offers a rigorous tool for designing strategies that promote consensus, limit fragmentation, or may regulate the impact of highly connected agents in public discourse. Overall, the finding of the present manuscript provides a modelling and computational setting for to analyse interventions in complex social systems where popularity, influence, and opinions co-evolve.

The paper is structured as follows. In Section 2, starting from a system of indistinguishable agents, we present the microscopic model for the evolution of the contacts. Such evolution is driven both by the desire of the agents to increase their followers once they enter the network and, consequently, gain more influence, but it also depends on how popular and endorsed are their opinions. In Section 2.1 we introduce the control variable for the evolution of the contacts and the optimal control problem linked to it. The objective of this control variable is to minimize the relative loss of the agent's contacts. We also present an interpretation of the optimal control functional as the continuous time limit of a discrete-time formulation. We conclude this section with the mean field description of the contacts evolution obtained through a suitable scaling of the contacts upgrade and the frequency of such evolution. Section 3 is devoted to the controlled evolution of the opinions. Again, we start from the microscopic multi-agent description of the binary interactions that shape each agent's opinion and present the optimal control problem linked to them. As we did for the evolution of the contacts, also for the opinion evolution we present the mean-field limit, leading to the Fokker-Planck-type equation for the time evolution of the joint density of opinions and contacts in the regime of small updates of the opinions and the contacts happening with a very high frequency. Finally, Section 4 presents a set of numerical experiments carried on using a Monte Carlo approach, that show the different outcomes of the joint contacts and opinion evolution under various possible configurations.

2 The evolutionary model for social network contacts

In this section we introduce the kinetic model governing the evolution of social media contacts. We first assume that agents' opinions are fixed, and we specify the microscopic interaction rules governing the evolution of each agent's number of connections. Following the approaches proposed in [5, 22], these rules lead to a Boltzmann-type master equation describing the evolution of the corresponding distribution.

Let us consider a population of indistinguishable interacting agents, each of them characterized, at each time $t \geq 0$, by its opinion $v \in [-1, 1]$ on a given topic, and by its contacts, which is the number of followers the agent has on a social media platform, that we will refer to as $c \geq 0$. Hence we consider the probability density of agents as $f = f(v, c, t)$ over the space of opinions and contacts at time $t > 0$, such that

$$\int_{[-1,1] \times \mathbb{R}_+} f(v, c, t) dv dc = 1,$$

and density marginals

$$h(c, t) := \int_{[-1,1]} f(v, c, t) dv, \quad g(v, t) := \int_{\mathbb{R}_+} f(v, c, t) dc.$$

We first analyze the evolution of agents' connection, considering the opinions as a fixed parameter. Thus, for any given measurable subset $D \subseteq \mathbb{R}_+$, the quantity

$$\int_D h(c, t) dc$$

represents the fraction of agents whose number of contacts satisfies $c \in D$ at time t .

As in [5], we assume that the agents are generally inclined to increase their number of social media followers once they enter the network, and that they tend to reach, at least, a certain number of followers \bar{c} , which represents a desirable popularity level. In addition, we assume that an agent's ability to acquire or retain contacts is influenced by the popularity of the opinion they express, so that opinion-driven visibility plays a direct role in the dynamics of the contact variable.

In practice, this leads to the following microscopic dynamics for the number of connections c of an agent with opinion v ,

$$c' = c - \beta \left(\Psi \left(\frac{c}{\bar{c}} \right) + \Phi(v) \right) c + \eta c, \quad (1)$$

where η is a random variable with zero mean and a finite standard deviation ν . Equation (1) models the fact that the evolution of the number of contacts is driven by three factors. The first one is deterministic and described by a

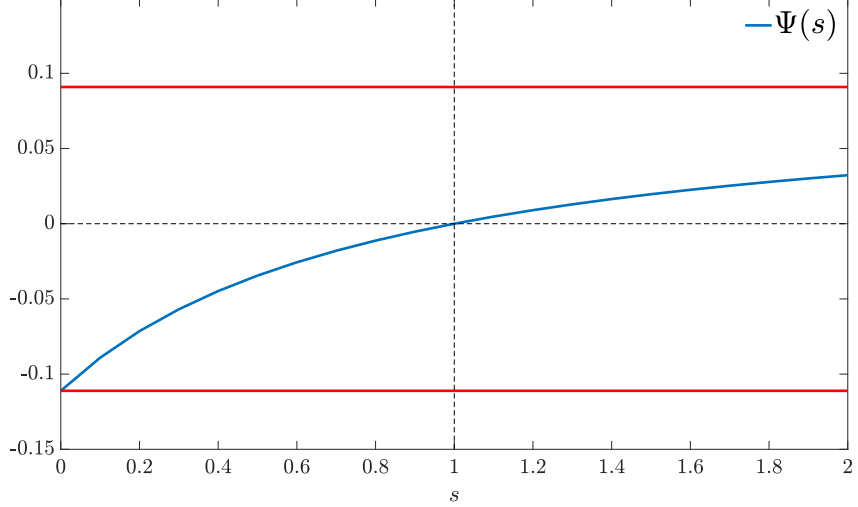


Figure 1: Plot of $\Psi(s)$. The red lines represent the bounds of the function when $\beta = 1$ and $\mu = 0.1$.

value function $\Psi(s)$ that we suppose defined as

$$\Psi(s) = \frac{1}{\beta} \left(\frac{\mu}{1-\mu} \right) \frac{s-1}{\frac{1+\mu}{1-\mu} s + 1},$$

with $s = c/\bar{c}$. This function is dimensionless, increasing and it is equal to zero at the reference point $s = 1$. Moreover, it is asymmetric: moving toward the reference level $s = 1$ is easier for agents starting below the threshold, while agents above the reference level face a weaker incentive to reduce their connections. This reflects the empirical principle that it is easier to gain new contacts when starting from a low number, whereas highly connected users are not motivated to decrease their popularity. This mechanism encodes the principles of the prospect theory formulated by Kahneman and Tversky [31]. The function is bounded by the values

$$-\frac{1}{\beta} \frac{\mu}{1-\mu} \leq \Psi(s) \leq \frac{1}{\beta} \frac{\mu}{1+\mu},$$

and it can be seen represented in Figure 1. This specific choice is justified by the results presented in [5].

The second contribution is also deterministic, it depends on the agent's opinion and it is represented by the function

$$\Phi(v) = \theta \left((v - m_v)^2 - \delta_\Phi^2 \right),$$

where $\theta > 0$, m_v is the mean opinion of the entire population and δ_Φ is a fixed parameter that depends on the tolerance of the population to unpopular opinions. This function is negative if the agent has an opinion with a distance which is less or equal than δ_Φ from the average opinion of the population, positive, and due to the compactness of the domain it is bounded in

$$-\theta \delta_\Phi^2 \leq \Phi(v) \leq \theta \left(4 - \delta_\Phi^2 \right).$$

Its role in (1) is to decrease the popularity of the ones who do not conform with the majority of the population, while increasing the number of connections of the ones with opinion close to the mean stance of the rest of the agents.

Finally, the third contribution to the evolution of the number of connections is a stochastic one, described by the random variable η , and modeling additional sources of influence. Since the domain of the variable c is \mathbb{R}_+ , one must ensure that η is bounded from below, in particular that

$$\eta \geq \frac{\beta \theta (4 - \delta_\Phi^2) (1 + \mu) - 1}{1 + \mu}.$$

2.1 The controlled evolution of social media contacts

We now introduce an external intervention mechanism aimed at regulating the evolution of an agent's popularity on the social network. To this aim, we modified the uncontrolled dynamics in (1) adding a control input κ so that

the microscopic evolution becomes

$$c' = c - \beta \left(\Psi \left(\frac{c}{\bar{c}} \right) + \Phi(v) - \kappa \right) c + \eta c. \quad (2)$$

The optimal control κ^* is obtained as the minimizer of the following cost functional

$$\kappa^* = \arg \min_{\kappa} \mathcal{J}[\kappa], \quad \mathcal{J}[\kappa] := \mathbb{E} \left[-\lambda \frac{c' - c}{c} R_c(c) H_c(v) + \frac{\gamma_c}{2} \kappa^2 \right], \quad (3)$$

which penalizes the relative loss of the agent's contacts along with a quadratic regularization term. Indeed, the quantity $(c' - c)/c$ is the incremental relative variation of contacts between two consecutive time steps, and overall the first term of \mathcal{J} promotes control actions capable of counterbalancing an expected loss of contacts, but only in the event that certain activation conditions are met. Specifically, such conditions are expressed by the activation functions $R_c(c)$ and $H_c(v)$. The parameter λ sets the intrinsic scale of the control action, determining the overall intensity with which contact growth can be enhanced relative to the natural dynamics. The second term appearing in the functional \mathcal{J} , meaning $\gamma_c \kappa^2/2$, penalizes the control magnitude, with the positive constant γ_c determining how costly it is to increase the number of contacts. The activation function $R_c(c)$ only depends on the current number of contacts of the agent and is modeled by the sigmoid

$$R_c(c) = \frac{1}{1 + \exp(-\alpha_R(c_{\min} - c))},$$

which is close to one when contacts fall below the threshold c_{\min} , and decreases as c grows beyond it. The activation function $H_c(v)$ depends instead on the local opinion density $m(v)$, it ensures that the control only acts on leaders positioned within a prescribed opinion region and is given by

$$H_c(v) = \frac{1}{1 + \exp(-\alpha_H(\rho(v) - \rho^*))},$$

which is increasing when the agent is surrounded by many others with similar opinions and models the phenomenon of social reinforcement. With $\rho(v)$ we indicate the *local opinion mass*, meaning

$$\rho(v) = \int_{|w-v| \leq r} f(w, c, t) dw dc,$$

i.e. the fraction of agents whose opinions have a distance from v which is less or equal than $r > 0$ in, while ρ^* indicates an activation threshold, meaning the minimum mass required for a significant group effect to be witnessed. The parameters $\alpha_R, \alpha_H > 0$ modify the steepness on the sigmoid functions. In this framework, $H_c(v)$ increases with the density of similar opinions, modeling the social tendency of the agents to seek more contacts when they feel part of a group with a shared vision.

The control model addresses the tendency to reduce the relative loss of popularity by acting when the number of agents' contacts decreases, while normalizing the action relative to the agent's current number of connections. Hence, the functional rewards any positive deviation of the contact dynamics from their uncontrolled evolution, that is, a positive relative increment of contacts. This enhancement is activated only for agents whose popularity level is below the desired threshold and whose opinion lies within the region where the intervention is intended to be active.

In order to obtain an explicit expression of the optimal control, for a single agent, we follow a greedy approach as in [4], looking for a low complexity computational representation of the optimal control problem expressed in (2)-(3) using the so-called model predictive control, that computes a suboptimal solution by iterating on a sequence of finite time steps. Here, we limit ourselves to a single evolution step, from c to c' , because we are interested in an instantaneous control strategies. For each agent, we can obtain an explicit expression of the optimal control deriving the functional $\mathcal{J}[\kappa]$ with respect to κ and setting the derivative equal to zero. Noticing that $\partial_{\kappa} c' = \beta c$, we get

$$\partial_{\kappa} \mathcal{J}[\kappa] = \mathbb{E}[-\lambda \beta R_c(c) H_c(v) + \gamma_c \kappa].$$

Imposing the first order optimality conditions $\partial_{\kappa} \mathcal{J}[\kappa] = 0$, recalling that $\mathbb{E}[\eta] = 0$, and using that $\gamma_c > 0$ we get

$$-\lambda \beta R_c(c) H_c(v) + \gamma_c \kappa = 0.$$

Finally, solving for κ yields the feedback control law

$$\kappa^* = \lambda \frac{\beta}{\gamma_c} R_c(c) H_c(v). \quad (4)$$

Remark 2.1. (Time discrete functional and continuous limit). We notice that the functional (3) can be interpreted as a one-step discrete-time functional. Indeed, introducing a partition of the time interval $[0, T]$, given by $t_n = n\Delta t$, $n = 0, \dots, N$, $N\Delta t = T$, with $\Delta t > 0$, we consider analogously with (3) the following discrete cost functional

$$\mathcal{J}_{\Delta t} = \sum_{n=0}^{N-1} \Delta t \mathcal{L}_n, \quad \mathcal{L}_n = -\lambda \frac{c^{n+1} - c^n}{\Delta t c^n} R_c(c^n) H_c(v^n) + \frac{\gamma_c}{2\Delta t} (\kappa^n)^2.$$

The factor $1/\Delta t$ inside the first term is introduced so that the first summand approximates the instantaneous relative growth rate as $\Delta t \rightarrow 0^+$ as follows

$$\frac{c^{n+1} - c^n}{\Delta t c^n} \approx \frac{\dot{c}(t_n)}{c(t_n)}.$$

Hence, letting $\Delta t \rightarrow 0^+$ we obtain the continuous functional

$$\mathcal{J}[\kappa] = \int_0^T \left[-\lambda \frac{\dot{c}(t)}{c(t)} R_c(c(t)) H_c(v(t)) + \frac{\tilde{\gamma}_c}{2} \kappa(t)^2 \right] dt. \quad (5)$$

where $\tilde{\gamma}_c$ is obtained by absorbing the Δt scaling of the discrete parameter γ_c .

Observe that the integrand contains the quantity \dot{c}/c . Formally we can write,

$$\int_0^T \frac{\dot{c}(t)}{c(t)} dt = \int_0^T d(\ln c(t)) = \ln c(T) - \ln c(0),$$

provided $c(t) > 0$ for all t and that the functions are regular enough. Therefore, if R_c and H_c were constant in time, or independent of c and v , the first integral in (5) would reduce to a boundary term:

$$-\lambda R_c H_c \int_0^T \frac{\dot{c}(t)}{c(t)} dt = -\lambda R_c H_c (\ln c(T) - \ln c(0)).$$

This shows that maximizing the integral of \dot{c}/c is equivalent, up to a multiplicative constant and boundary terms, to maximizing the logarithmic growth of contacts over the time window $[0, T]$.

The Fokker-Planck type equation for the kinetic evolution of contacts

In order to pass to a mean field description of contacts, we suppose that the process of network formation is the result of small increments of the number of connections of the agents. This translates in the scaling of equation (2), taking Let $\varepsilon > 0$, the scaled equation now reads

$$c' = c - \varepsilon \beta \left(\Psi^\varepsilon \left(\frac{c}{\bar{c}} \right) + \Phi(v) - \kappa \right) c + \eta_\varepsilon c$$

where η_ε is a random variable with mean equal to zero and standard deviation $\sqrt{\varepsilon} \nu$, while the value function Ψ^ε is defined as

$$\Psi^\varepsilon(s) = \frac{1}{\beta \varepsilon} \left(\frac{\mu}{1-\mu} \right) \frac{s^\varepsilon - 1}{\frac{1+\mu}{1-\mu} s^\varepsilon + 1},$$

and the scaled control is the same as in (4), since we both scale β and γ_c with the same variable ε .

Supposing v fixed, we can now derive an evolutionary model for the controlled formation of the network. The rescaled density of the connections, $h_\varepsilon(v, c)$, obeys a Boltzmann-like equation of the form

$$\partial_t \int_{\mathbb{R}_+} \varphi(c) h_\varepsilon(v, c) dc = \mathbb{E} \left[\int_{\mathbb{R}_+} \chi(c) (\varphi(c') - \varphi(c)) h_\varepsilon(v, c) dc \right], \quad (6)$$

where φ is a test function and χ is the frequency of interaction, which we suppose to be very high, specifically we set it to be equal to $\chi(c) = 1/\varepsilon$. Notice that the choice $\varphi(c) = 1$ leads to the conservation of the total mass of the agents, while other choices give us other information on the network evolution, for example setting $\varphi(c) = c$ leads to the evolution of the mean number of connections which we can see is not conserved in time. Assuming φ smooth enough we can use its Taylor expansions to simplify the expression in (6). We have that

$$\mathbb{E} [c' - c] = \varepsilon \beta \left(\Psi^\varepsilon \left(\frac{c}{\bar{c}} \right) + \Phi(v) - \kappa \right) c, \quad (7)$$

and

$$\mathbb{E} [(c' - c)^2] = \varepsilon^2 \beta^2 \left(\Psi^\varepsilon \left(\frac{c}{\bar{c}} \right) + \Phi(v) - \kappa \right)^2 c^2 + \varepsilon \nu^2 c^2, \quad (8)$$

while for the cubic increments we have

$$\begin{aligned}\mathbb{E}[(c' - c)^3] &= \varepsilon^3 \beta^3 \left(\Psi^\varepsilon \left(\frac{c}{\bar{c}} \right) + \Phi(v) - \kappa \right)^3 c^3 + \mathbb{E}[\eta_\varepsilon^3] c^3 \\ &\quad + 3\varepsilon^2 \beta \nu^2 \left(\Psi^\varepsilon \left(\frac{c}{\bar{c}} \right) + \Phi(v) - \kappa \right) c^3.\end{aligned}\tag{9}$$

This results in

$$\begin{aligned}\partial_t \int_{\mathbb{R}_+} \varphi(c) h_\varepsilon(v, c) dc &= \int_{\mathbb{R}_+} \left(\varphi'(c) \beta \left(\Psi^\varepsilon \left(\frac{c}{\bar{c}} \right) + \Phi(v) - \kappa \right) c + \frac{\nu^2 c^2}{2} \varphi''(c) \right) h_\varepsilon(v, c) dc \\ &\quad + \varepsilon \int_{\mathbb{R}_+} \left(\frac{\varepsilon \beta^2}{2} \left(\Psi^\varepsilon \left(\frac{c}{\bar{c}} \right) + \Phi(v) - \kappa \right)^2 c^2 \varphi''(c) \right) h_\varepsilon(v, c) dc \\ &\quad + O(\varepsilon^2).\end{aligned}$$

Now letting $\varepsilon \rightarrow 0$, noticing that

$$\lim_{\varepsilon \rightarrow 0} \Psi^\varepsilon \left(\frac{c}{\bar{c}} \right) = \frac{\mu}{2} \ln \left(\frac{c}{\bar{c}} \right)$$

and using the notation $h(v, c)$ for the limit of $h_\varepsilon(v, c)$ as $\varepsilon \rightarrow 0$, we get the following simplified expression for the evolution of the density of the controlled connections

$$\partial_t \int_{\mathbb{R}_+} \varphi(c) h(v, c) dc = \int_{\mathbb{R}_+} \left(\varphi'(c) \beta \left(\frac{\mu}{2} \ln \left(\frac{c}{\bar{c}} \right) + \Phi(v) - \lambda \frac{\beta}{\gamma_c} R_c(c) H_c(v) \right) c + \frac{\nu^2 c^2}{2} \varphi''(c) \right) h(v, c) dc,$$

which is the weak form of the following Fokker-Planck equation for h

$$\partial_t h(v, c) = -\partial_c \left(\beta h(v, c) \left(\frac{\mu}{2} \ln \left(\frac{c}{\bar{c}} \right) + \Phi(v) - \lambda \frac{\beta}{\gamma_c} R_c(c) H_c(v) \right) c - \frac{\nu^2}{2} \partial_c (c^2 h(v, c)) \right). \tag{10}$$

3 The controlled opinion evolution

In this section, we focus on the evolution of opinions, represented by a continuous variable $v \in [-1, 1]$, where -1 indicates a strongly negative idea on a given topic, while $+1$ signifies a strongly positive one.

Consider two interacting agents with pre-interaction opinions v, v_* and contact levels c, c_* . We denote by v', v'_* the corresponding post-interaction opinions, which evolve through binary interactions, which depends on deterministic and stochastic factors, of the form

$$\begin{aligned}v' &= v + \alpha (P(v, v_*, c, c_*) (v_* - v) + u) + D(v) \xi, \\ v'_* &= v_* + \alpha (P(v_*, v, c_*, c) (v - v_*) + u_*) + D(v_*) \xi_*.\end{aligned}\tag{11}$$

The random part is given by some unpredictable fluctuation in the opinion which is due, for example, to the agent's access to information through the news, and is modeled by a random variable ξ with mean equal to zero and given finite standard deviation σ . This variable is weighted by a self diffusion function $D(v) = 1 - v^2$ that is equal to zero at the boundary of the domain $[-1, 1]$.

The deterministic part of the interaction is modeled by the compromise function $P(v, v_*, c, c_*)$, which depends on the opinions of the agents interacting and on their number of connections. The strength of this exchange is expected to be stronger when the two opinions v and v_* are close to each other, and when the influence associated with one individual's connectivity exceeds that of the other. This can be mathematically modeled by expressing the compromise function as the product of two functions

$$P(v, v_*, c, c_*) = H(v, v_*) K(c, c_*),$$

where

$$H(v, v_*) = \mathbf{1}_{\{|v - v_*| < \delta\}}, \quad \delta > 0,$$

restricts the interactions to agents with sufficiently close opinions, and

$$K(c, c_*) = \frac{c_*^p}{c^p + c_*^p}$$

weights the relative influence of connectivity, with $p > 0$.

The other deterministic factor is given by the control input u . Here, we denote by u^* the optimal control obtained as the minimizer of the quadratic cost functional defined by

$$u^* = \arg \min_u \mathcal{V}[u], \quad \mathcal{V}[u] = \mathbb{E} \left[\frac{1}{2} (v' - \tilde{v})^2 R_v(c) H_v(v) + \frac{\gamma_v}{2} \alpha u^2 \right].$$

The functional \mathcal{V} balances two competing effects. The first term measures the deviation of the post-interaction opinion v' from a prescribed target value \tilde{v} , that we can suppose is depending on the initial distribution, i.e., $\tilde{v} = \tilde{v}(v_0)$, and is weighted by the activation functions $R_v(c)$ and $H_v(v)$, which restrict the action of the control to agents that are both sufficiently active in terms of contacts and lie in a relevant opinion region. The second term penalizes the control magnitude through the parameter $\gamma_v > 0$, ensuring that excessively strong interventions are discouraged.

Overall, the optimal feedback control u^* tends to steer the opinion toward the target one \tilde{v} , but only when the activation conditions encoded by $R_v(c)$ and $H_v(v)$ are satisfied. The choices for such activation functions will be described in Section 4. We are now interested in an explicit expression for the control u_i^* . First, we derive $\mathcal{V}[u]$ in u , noticing that $\partial_u v' = \alpha$, and we get

$$\partial_u \mathcal{V}[u] = \mathbb{E}[(v' - \tilde{v}) \alpha R_v(c) H_v(v) + \gamma_v \alpha u]$$

Then, imposing $\partial_u \mathcal{V}[u] = 0$ and simplifying $\alpha > 0$, we substitute the expression of v' and we pass to the expected value taking into account the fact that the random variable ξ is centered in zero. In the end, we obtain

$$(v + \alpha(P(v, v_*, c, c_*)(v_* - v) + u) - \tilde{v}) R_v(c) H_v(v) + \gamma_v u = 0.$$

Solving for u yields

$$u^* = - \frac{R_v(c) H_v(v) [v + \alpha(P(v, v_*, c, c_*)(v_* - v)) - \tilde{v}]}{\gamma_v + \alpha R_v(c) H_v(v)}.$$

The Fokker-Planck type equation for the kinetic evolution of opinions

Also in the opinion case, just like we did for the contacts in Section 2.1, we can assume that the opinion evolution is due to small changes of the opinions happening with a high frequency. To this aim, we scale the opinion exchange intensity using a small positive parameter ε . Suppose agent i has the pre-interaction couple of opinion and contacts given by (v, c) , while the agent j has opinion and contacts given by (v_*, c_*) , the scaled version of the binary interaction (11) reads as

$$\begin{cases} v' = v + \varepsilon \alpha (P(v, v_*, c, c_*) (v_* - v) + u) + D(v) \xi^\varepsilon, \\ v'_* = v_* + \varepsilon \alpha (P(v_*, v, c_*, c) (v - v_*) + u_*) + D(v_*) \xi_*^\varepsilon, \end{cases}$$

with $\xi^\varepsilon, \xi_*^\varepsilon$ random variables with mean equal to zero and variance $\mathbb{E}[(\xi^\varepsilon)^2] = \mathbb{E}[(\xi_*^\varepsilon)^2] = \varepsilon \sigma^2$. The scaled density of opinion and contacts $f_\varepsilon(v, c, t)$ verifies the following Boltzmann-type equation

$$\begin{aligned} \partial_t \int_{\mathbb{R}_+} \int_{-1}^1 f_\varepsilon(v, c, t) \varphi(v, c) dv dc &= \frac{1}{2} \mathbb{E} \left[\int_{\mathbb{R}_+^2} \int_{[-1,1]^2} (\varphi(v', c') + \varphi(v'_*, c'_*) \right. \\ &\quad \left. - \varphi(v, c) - \varphi(v_*, c_*)) f_\varepsilon(v, c, t) f_\varepsilon(v_*, c_*, t) dv dv_* dc dc_* \right], \end{aligned} \tag{12}$$

with $\varphi(v, c)$ smooth test function. In order to write a simplified expression of (12) we compute the Taylor expansions up to order three of both $\varphi(v', c')$ and $\varphi(v'_*, c'_*)$ around v and v_* , respectively. To do so, we compute the increments

$$\begin{aligned} \mathbb{E}[v' - v] &= \varepsilon \alpha (P(v, v_*, c, c_*) (v_* - v) + u), \\ \mathbb{E}[(v' - v)^2] &= \varepsilon^2 \alpha^2 (P(v, v_*, c, c_*) (v_* - v) + u)^2 + \varepsilon \sigma^2 D(v)^2, \end{aligned}$$

and

$$\begin{aligned} \mathbb{E}[(v' - v)^3] &= \varepsilon^3 \alpha^3 (P(v, v_*, c, c_*) (v_* - v) + u)^3 + \mathbb{E}[(D(v) \xi^\varepsilon)^3] \\ &\quad + 3 \varepsilon^2 \alpha \sigma^2 D(v)^2 (P(v, v_*, c, c_*) (v_* - v) + u). \end{aligned}$$

Taking into consideration also (7), (8), and (9), and using them in (12) we get

$$\begin{aligned} \partial_t \int_{\mathbb{R}_+} \int_{-1}^1 f_\varepsilon(v, c, t) \varphi(v, c) dv dc &= \varepsilon \int_{\mathbb{R}_+} \int_{-1}^1 (\alpha \partial_v \varphi(v, c) (\mathcal{P}[f_\varepsilon](v, c, t) + u) + \\ &+ \partial_c \varphi(v, c) \beta \left(\Psi^\varepsilon \left(\frac{c}{\varepsilon} \right) + \Phi(v) - \kappa \right) c \\ &+ \partial_{vv}^2 \varphi(v, c) \frac{\sigma^2 D(v)^2}{2} \\ &+ \partial_{cc}^2 \varphi(v_*, c_*) \frac{v^2 c^2}{2} \right) f_\varepsilon(v, c, t) dv dc + \mathcal{R}(\varepsilon), \end{aligned} \quad (13)$$

where the reminder $\mathcal{R}(\varepsilon) = O(\varepsilon^2)$ and the nonlocal operator $\mathcal{P}[f_\varepsilon]$ is defined as

$$\mathcal{P}[f_\varepsilon](v, c, t) = \int_{\mathbb{R}_+} \int_{-1}^1 P(v, v_*, c, c_*) (v_* - v) f_\varepsilon(v_*, c, t) dv_* dc_*.$$

To model the higher frequency of interaction we can scale the time variable using the same scaling parameter ε , leading to the scaling $t \rightarrow \varepsilon t$. Now, we let $\varepsilon \rightarrow 0$: for the control variable we have that

$$\lim_{\varepsilon \rightarrow 0} u = - \frac{R_v(c) H_v(\rho(v)) [v - \tilde{v}]}{\gamma_v},$$

and using the notation $f(v, c, t)$ for the limit of $f_\varepsilon(v, c, t)$ when $\varepsilon \rightarrow 0$ we have that equation (13) tends to

$$\begin{aligned} \partial_t \int_{\mathbb{R}_+} \int_{-1}^1 f(v, c, t) \varphi(v, c) dv dc &= \int_{\mathbb{R}_+} \int_{-1}^1 (\alpha \partial_v \varphi(v, c) (\mathcal{P}[f](v, c, t) + \\ &+ \frac{R_v(c) H_v(\rho(v)) (v - \tilde{v})}{\gamma_v}) + \partial_c \varphi(v, c) \beta \left(\frac{\mu}{2} \ln \left(\frac{c}{\tilde{c}} \right) + \Phi(v) - \lambda \frac{\beta}{\gamma_c} R_c(c) H_c(v) \right) c \\ &+ \partial_{vv}^2 \varphi(v, c) \frac{\sigma^2 D(v)^2}{2} + \partial_{cc}^2 \varphi(v_*, c_*) \frac{v^2 c^2}{2} \right) f(v, c, t) dv dc, \end{aligned}$$

which is the weak form of the following Fokker-Planck equation

$$\begin{aligned} \partial_t f(v, c, t) &= -\alpha \partial_v \left(\left(\mathcal{P}[f](v, c, t) + \frac{R_v(c) H_v(\rho(v)) (v - \tilde{v})}{\gamma_v} \right) f(v, c, t) \right) \\ &- \beta \partial_c \left(\left(\frac{\mu}{2} \ln \left(\frac{c}{\tilde{c}} \right) + \Phi(v) - \lambda \frac{\beta}{\gamma_c} R_c(c) H_c(v) \right) c f(v, c, t) \right) \\ &+ \frac{\sigma^2}{2} \partial_{vv}^2 \left(D(v)^2 f(v, c, t) \right) + \frac{v^2}{2} \partial_{cc}^2 \left(c^2 f(v, c, t) \right). \end{aligned} \quad (14)$$

4 Numerical experiments

In this Section we present a set of numerical experiments aimed at illustrating the behavior of the proposed model and analyzing the joint evolution of contacts and opinions when the control mechanisms introduced in the previous sections are active.

For the numerical approximation of the Boltzmann-type equation (6) in the Fokker-Planck regime (10)–(14), we adopt a Monte Carlo-type strategy. In particular, we rely on an asymptotic stochastic particle method suitable for kinetic equations in the quasi-invariant limit, introducing the discrete update

$$f^{n+1} = \left(1 - \frac{\Delta t}{\varepsilon} \right) f^n + \frac{\Delta t}{\varepsilon} \mathcal{G}_\varepsilon(f^n, f^n), \quad (15)$$

where the gain operator \mathcal{G}_ε accounts for the inflow of particles at position (v, c) at time t after the interaction rules (2) and (11) are applied.

The particle scheme used to simulate (15) is detailed in Algorithm 1, where we take $\varepsilon = \Delta t$ for simplicity. Further details on this class of asymptotic particle methods can be found, e.g., in [34].

Algorithm 1 Asymptotic particle-based scheme (Nanbu-like algorithm)

Fix $0 < \varepsilon = \Delta t < 1$ and N_s .

Sample $\{v_i^0, c_i^0\}_{i=1}^{N_s}$ from the initial distribution $f_0(v, c)$.

for $n = 0 : N_t - 1$ **do**

 Set $N_c = \text{round}(N_s/2)$.

 Select N_c unordered random pairs (i, i_*) uniformly without repetition.

for $k = 1 : N_c$ **do**

 Let (i, i_*) be the k -th selected pair.

 Sample noise terms $\eta_{\varepsilon, i}^n, \eta_{\varepsilon, i_*}^n$ with $\langle \eta \rangle = 0$, $\langle \eta^2 \rangle = \varepsilon v^2$, and $\xi_i^n, \xi_{i_*}^n \sim \mathcal{N}(0, 1)$.

 Compute the contact-control contributions

$$\kappa_j^n = \lambda \frac{\beta}{\gamma_c} R_c(c_j^n) H_c(v_j^n), \quad j \in \{i, i_*\}.$$

 Compute the opinion controls

$$u_i^n = -\frac{R_v(c_i^n) H_v(v_i^n) \left(v_i^n + \varepsilon \alpha (P(v_i^n, v_{i_*}^n, c_i^n, c_{i_*}^n) (v_{i_*}^n - v_i^n)) - \tilde{v} \right)}{\gamma_v + \varepsilon \alpha R_v(c_i^n) H_v(v_i^n)},$$

$$u_{i_*}^n = -\frac{R_v(c_{i_*}^n) H_v(v_{i_*}^n) \left(v_{i_*}^n + \varepsilon \alpha (P(v_{i_*}^n, v_i^n, c_{i_*}^n, c_i^n) (v_i^n - v_{i_*}^n)) - \tilde{v} \right)}{\gamma_v + \varepsilon \alpha R_v(c_{i_*}^n) H_v(v_{i_*}^n)}.$$

 Update contacts

$$c_j^{n+1} = c_j^n - \varepsilon \beta \left(\Psi^\varepsilon \left(\frac{c_j^n}{\bar{c}} \right) + \Phi(v_j^n) - \kappa_j^n \right) c_j^n + \eta_{\varepsilon, j}^n c_j^n, \quad j \in \{i, i_*\}.$$

 Update opinions

$$v_i^{n+1} = v_i^n + \varepsilon \alpha \left(P(v_i^n, v_{i_*}^n, c_i^n, c_{i_*}^n) + u_i^n \right) + \sqrt{\varepsilon} \sigma D(v_i^n) \xi_i^n,$$

$$v_{i_*}^{n+1} = v_{i_*}^n + \varepsilon \alpha \left(P(v_{i_*}^n, v_i^n, c_{i_*}^n, c_i^n) + u_{i_*}^n \right) + \sqrt{\varepsilon} \sigma D(v_{i_*}^n) \xi_{i_*}^n.$$

end for
end for

Table 1: Summary of model parameters.

Parameter	Value
Contacts dynamics	
Interaction strength	$\beta = 1$
Endogenous modulation $\Psi(\cdot)$	$\mu = 0, \bar{c} = 200$
Endogenous modulation $\Phi(\cdot)$	$\theta = 2, \delta_\Phi = 0.1$
Contacts noise	$\eta, \nu = 0.1$
Contact control κ^*	
Cost penalization	$\gamma_c = 1$
Maximal control intensity	$\lambda = 1$
Activation thresholds	$\alpha_R = \alpha_H = 0.1, r = 0.7, \rho^* = 0.5$
Contact activation level	$c_{\min} = 100$
Opinion dynamics	
Binary interaction	$\alpha = 1, \delta = 0.8, p = 3, \tilde{v} = 0.5$
Opinions noise	$\xi, \sigma = 0.1$
Opinion control u^*	
Cost penalization	$\gamma_v = 10$
Thresholds	$R_v(c) = H_v(v) = 1$

4.1 Test 1: comparative analysis of control strategies in coupled contact–opinion dynamics

In this test we investigate the role of contact and opinion control mechanisms in a structured “leader–follower” system, where leaders denote agents endowed with control authority (or externally driven dynamics), while followers are agents that evolve according to interaction rules and respond to the influence of the leaders.

We consider a population of agents, 25% of which are designated as “leaders”, whereas the other represent the “mass”. The simulation runs up to a final time $T = 50$ with uniform time step $\Delta t = 10^{-3}$, and the all the others parameters used in this test are listed in Tab. 1.

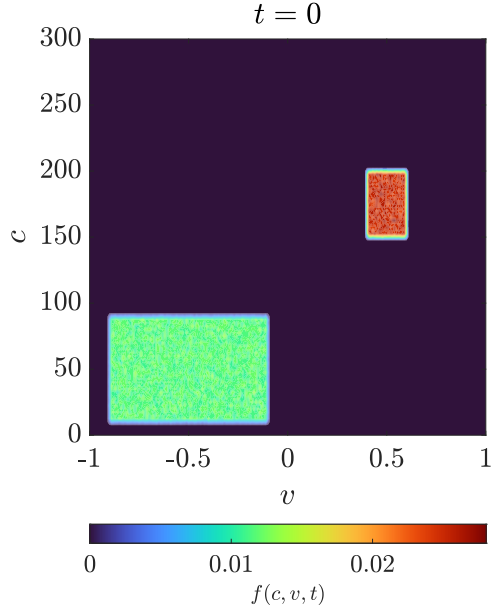


Figure 2: Test 1. Joint density $f(c, v, 0)$ at the initial time.

We sample $N_s = 10^6$ agents to simulate the model. At the initial time $t = 0$, the joint density $f_0(c, v) = f(c, v, 0)$ is represented in Fig. 2, and is provided as follows: the leaders’ states (c, v) are sampled from a continuous uniform distribution $(c, v) \sim \text{Unif}([150, 200] \times [0.4, 0.6])$, representing a cohesive and highly connected group with an opinion significantly different from that of the mass, which instead is initialized according to $(c, v) \sim$

$\text{Unif}([10, 90] \times [-0.9, -0.1])$, corresponding to a low-connectivity population spread over a broad range of opinions.

We examine four scenarios: (a) fully uncontrolled dynamics; (b) contact control κ^* active only for leaders; (c) opinion control u^* active only for leaders; (d) both controls simultaneously active on leaders.

Simulation results are reported in Fig. 3, which displays snapshots of the joint density $f(c, v, t)$ at selected times for each scenario, and in Fig. 4, illustrating the temporal evolution of the marginal distributions of contacts $h(c)$ and opinions $g(v)$.

In the uncontrolled case (a), the leader group, initially located around an extreme opinion, progressively loses contacts, thereby reducing its influence, and is eventually absorbed into the followers' cluster, converging to a compromise opinion. In scenario (b), leaders initially lose popularity, but the contact control activates near the threshold c_{\min} , preventing collapse and enabling them to regain influence; as a result, the overall opinion shifts toward a compromise closer to the leaders' initial stance. Scenario (c), with only opinion control active, shows that the loss of contacts dominates the dynamics: leaders rapidly lose influence and merge into the followers' distribution, again converging to a compromise. Finally, in scenario (d), the combined action of both controls preserves leaders' popularity and enables them to steer the population toward their target opinion.

In Figure 5 we report the time evolution of the mean number of contacts $m_c(t)$ and of the mean opinion $m_v(t)$ for the four scenarios (a)–(d). The plots show that when the contact control is active, namely in scenarios (b) and (d), the global mean of contacts exhibits a sustained growth over time, counteracting the natural decay produced by the uncontrolled dynamics. Moreover, in scenario (d), where both opinion and contact controls are simultaneously activated, the combined action of the two control layers drives the population's mean opinion towards the target value promoted by the leader group, highlighting the synergistic effect of the coupled control mechanisms.

This test highlights how influence depends on visibility. When leaders let their popularity decay, their capacity to shape collective opinion quickly disappears, and they are reabsorbed into the majority view. Maintaining contacts prevents this loss of visibility, allowing leaders to maintain a role in directing the opinion landscape. The combination of preserving visibility and exerting persuasive effort produces lasting influence, in this case persuasion alone is ineffective when the audience becomes too small.

4.2 Test 2: leader-driven opinion steering: symmetric vs. asymmetric competition

In this test we study the effect of opinion control in a social system consisting of two competing leader groups, each promoting an opposite opinion, and a third uncontrolled group representing the mass of followers. The aim is to analyse how symmetric or asymmetric penalization of the opinion-control effort influences the outcome of the competition for consensus.

We consider a population of agents divided as follows: 25% constitute Leader Group A, another 25% constitute Leader Group B, and the remaining 50% form the follower population: the “mass”. The simulation horizon is $T = 50$ with time step $\Delta t = 10^{-3}$.

The evolution of contacts and opinions follows the same parameters used in Test 1 as in Tab 1. The only difference concerns the penalization parameters for the opinion control, denoted here by γ_v^A and γ_v^B for the two leader groups, and for the target opinions \tilde{v}_A, \tilde{v}_B .

In Fig. 6 we report the initial datum $f_0(c, v)$, sampled from $N_s = 10^6$ agents. At the initial time $t = 0$, leaders of Group A are sampled from $(c, v) \sim \text{Unif}([200, 250] \times [-0.6, -0.4])$, with a target opinion $\tilde{v}_A = -0.5$, representing a highly connected group promoting a moderately negative opinion. Leaders of Group B are sampled from $(c, v) \sim \text{Unif}([200, 250] \times [0.4, 0.6])$, and similarly promote a positive target opinion $\tilde{v}_B = 0.5$. Followers are initialized according to $(c, v) \sim \text{Unif}([50, 100] \times [-0.8, 0.8])$, thus representing a poorly connected population spread across a wide range of opinions.

We analyse three scenarios: (a) no control: both leader groups evolve freely under the uncontrolled opinion dynamics; (b) symmetric control: both leader groups employ the optimal opinion-control strategy with identical penalization, $\gamma_v^A = \gamma_v^B = 1$; (c) asymmetric control: group A faces a much higher penalization, $\gamma_v^A = 100$, while group B keeps $\gamma_v^B = 1$.

Simulation results are presented in Fig. 7, showing snapshots of the joint density $f(c, v, t)$ at selected times, and in Fig. 8, illustrating the evolution of the marginal distributions of contacts $h(c)$ and opinions $g(v)$.

In the uncontrolled case (a), leaders in both groups progressively lose influence due to contact decay and are unable to maintain their initial stance. Their opinions converge toward a compromise around zero, reflecting the symmetry of the initial configuration. In scenario (b), where both groups have the same control strength, leaders succeed in maintaining their respective target opinions. The follower population is simultaneously attracted toward both opinion poles, resulting in a persistent polarization and the emergence of a stable central cluster. Owing to symmetry, this central group remains approximately stationary and is not significantly attracted by either side. In the asymmetric scenario (c), the stronger penalization of Group A makes its leaders less effective at sustaining

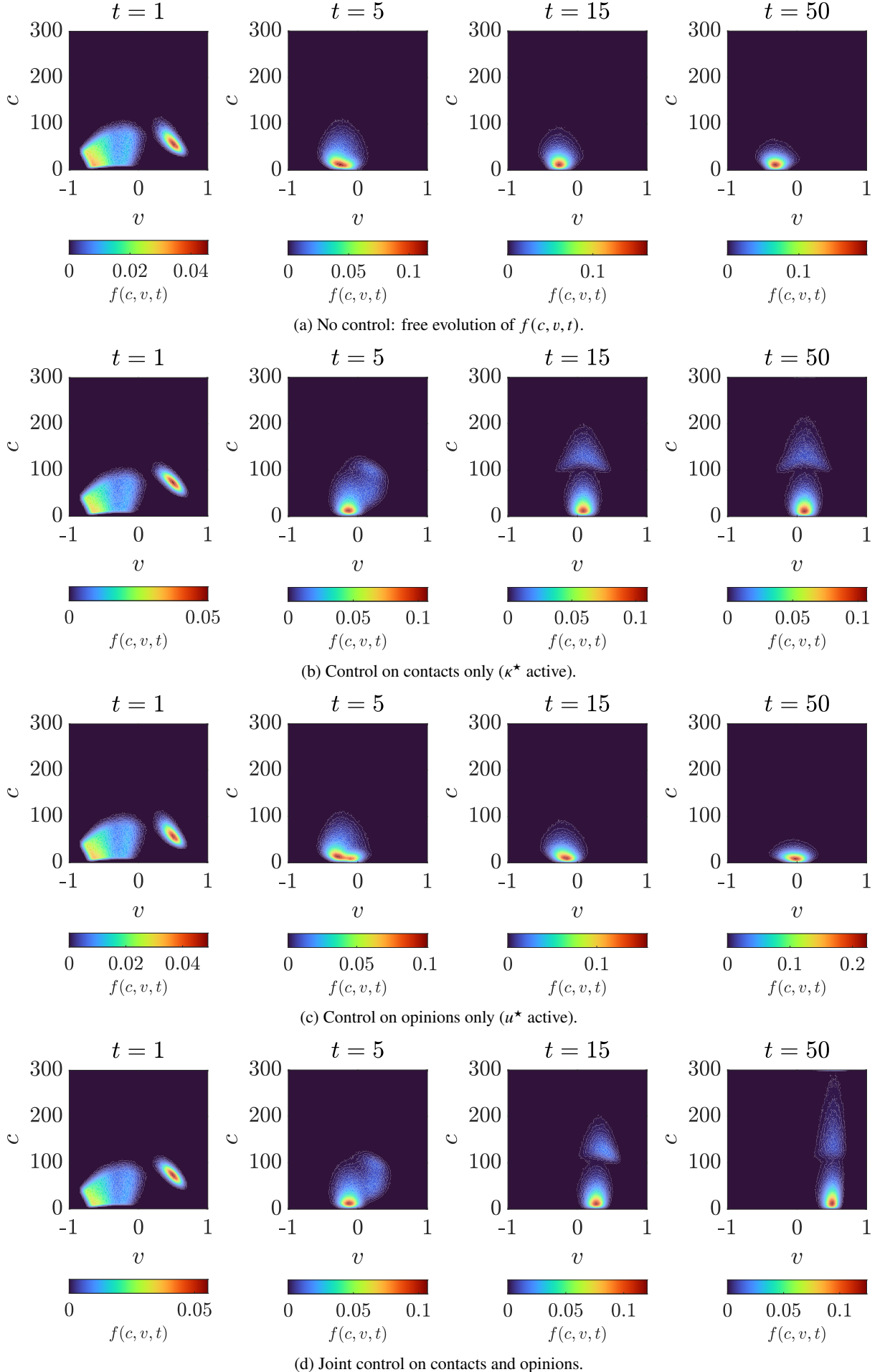


Figure 3: Test 1. Time evolution of the joint density $f(c, v, t)$ in the (v, c) plane for different control strategies. Each panel shows snapshots at times $t = 1, 5, 50$. (a) uncontrolled dynamics; (b) control on contacts; (c) control on opinions; (d) both controls active.

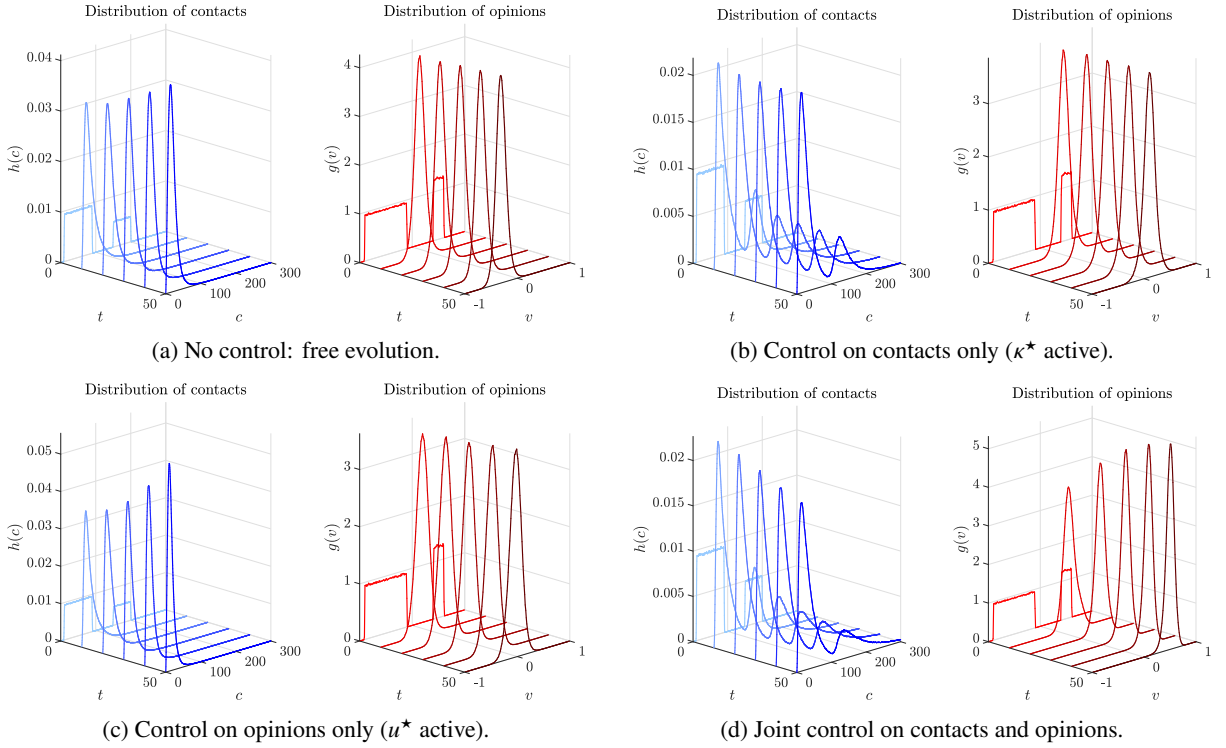


Figure 4: Test 1. Time evolution of the marginal distributions of contacts and opinions at different times for different control strategies. Each panel shows both distributions together: contacts (left) and opinions (right). (a) uncontrolled dynamics; (b) control on contacts; (c) control on opinions; (d) both controls active.

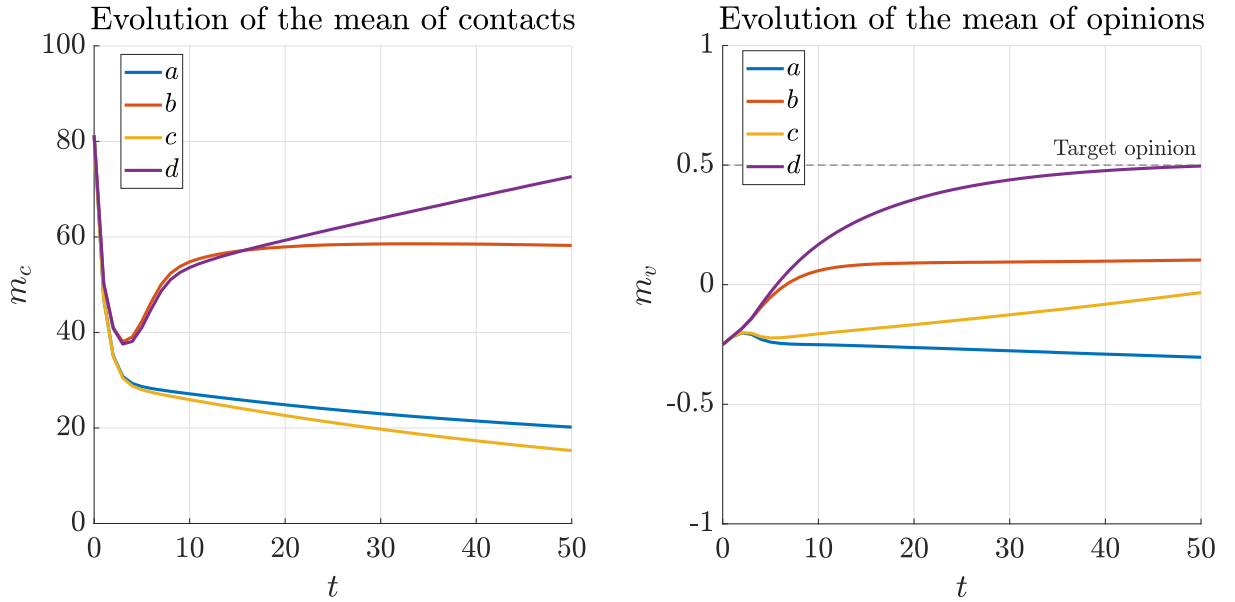


Figure 5: Test 1. Time evolution of the mean number of contacts $m_c(t)$ (left panel) and the mean opinion $m_v(t)$ (right panel) over the interval $[0, T]$. In both panels we report the temporal averages corresponding to the four scenarios (a)–(d), each represented with a different colour.

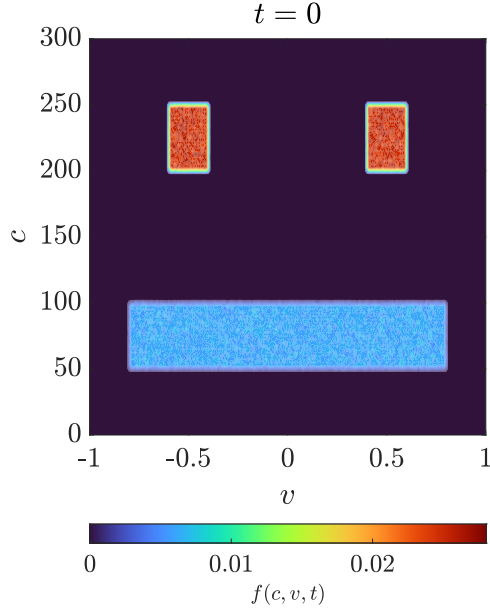


Figure 6: Test 2. Joint density $f(c, v, 0)$ at the initial time.

their target opinion, whereas Group B, with a lower penalization, maintains a strong control action. Consequently, Group B successfully drives the entire follower population toward its own target opinion, eventually dominating the competition for consensus.

In this test we see how competition between elite groups depends on the balance of resources devoted to persuasion. If neither side sustains its effort, both lose visibility and the population drifts toward a centrist consensus. Equal control efforts stabilise a polarized environment, with two enduring opinion poles and a persistent centre. When resources are asymmetric, the better-supported group dominates: unequal persuasive capacity translates into unequal influence over public opinion.

4.3 Test 3: emergence of echo chambers under local contact control

In this test we analyse a setting in which two groups of leaders, characterised by markedly opposite opinions, interact with a large population of followers whose initial opinions are closer to one of the two leader groups. The aim is to study how local control of contacts performed by one or both leader groups affects the formation of echo chambers and the eventual opinion distribution of the mass.

The total population consists of interacting agents, with 25% assigned to Leader Group A, 25% to Leader Group B, and the remaining 50% form the follower population. The simulation horizon is $T = 150$ with time step $\Delta t = 10^{-3}$.

The dynamics of contacts and opinions evolve according to the parameters reported in Table 1, here with penalization weights $\gamma_c = \gamma_v = 1$.

The initial joint density $f_0(c, v)$, sampled from $N_s = 10^6$ agents, is illustrated in Fig. 9. At time $t = 0$, leaders of Group A are sampled from $(c, v) \sim \text{Unif}([200, 250] \times [-0.6, -0.4])$, and are associated with the target opinion $\tilde{v}_A = -0.5$, representing a highly connected community endorsing a moderately negative stance. Leaders of Group B are initialised as $(c, v) \sim \text{Unif}([200, 250] \times [0.4, 0.6])$, with a corresponding positive target opinion $\tilde{v}_B = 0.5$. Followers are drawn from $(c, v) \sim \text{Unif}([50, 100] \times [0.1, 0.6])$, representing a poorly connected and more heterogeneous population.

We compare three configurations of the control dynamics. In the first one, only the opinion control u^* is active for the two leader groups. In the second configuration, both groups employ the opinion control, while Group A also activates the contact control κ^* . In the third configuration, both controls are active for both leader groups.

The results, displayed in Fig. 10 through snapshots of the joint density $f(c, v, t)$, and in Fig. 11 via the evolution of the marginal distributions of contacts $h(c)$ and opinions $g(v)$, reveal a clear differentiation among the three scenarios. In all cases, both leader groups initially experience a decline in their number of contacts due to the endogenous mechanisms governing the contact dynamics. When only the opinion control is active, this decay leads to a strong weakening of both leader groups, and the followers tend to preserve their initial opinion distribution. When Group A activates the contact control, however, the decline of its connectivity is mitigated and a cohesive cluster emerges around its target opinion; this cluster progressively attracts both the follower population and,

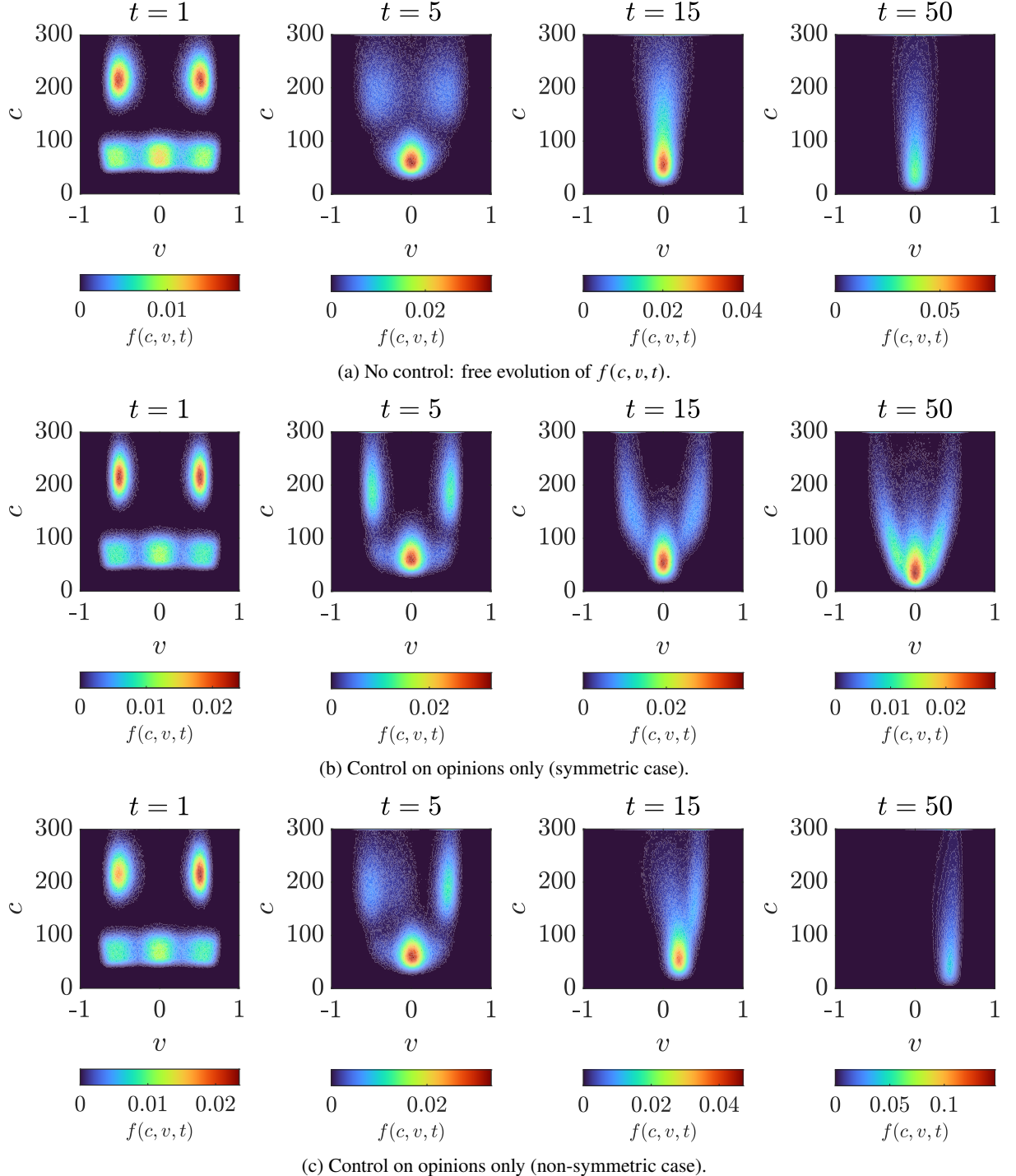


Figure 7: Test 2. Time evolution of the joint density $f(c, v, t)$ in the (v, c) plane. Each panel shows snapshots at times $t = 1, 5, 10, 15, 20$. (a) uncontrolled dynamics; (b) symmetric opinion control; (c) non-symmetric opinion control.

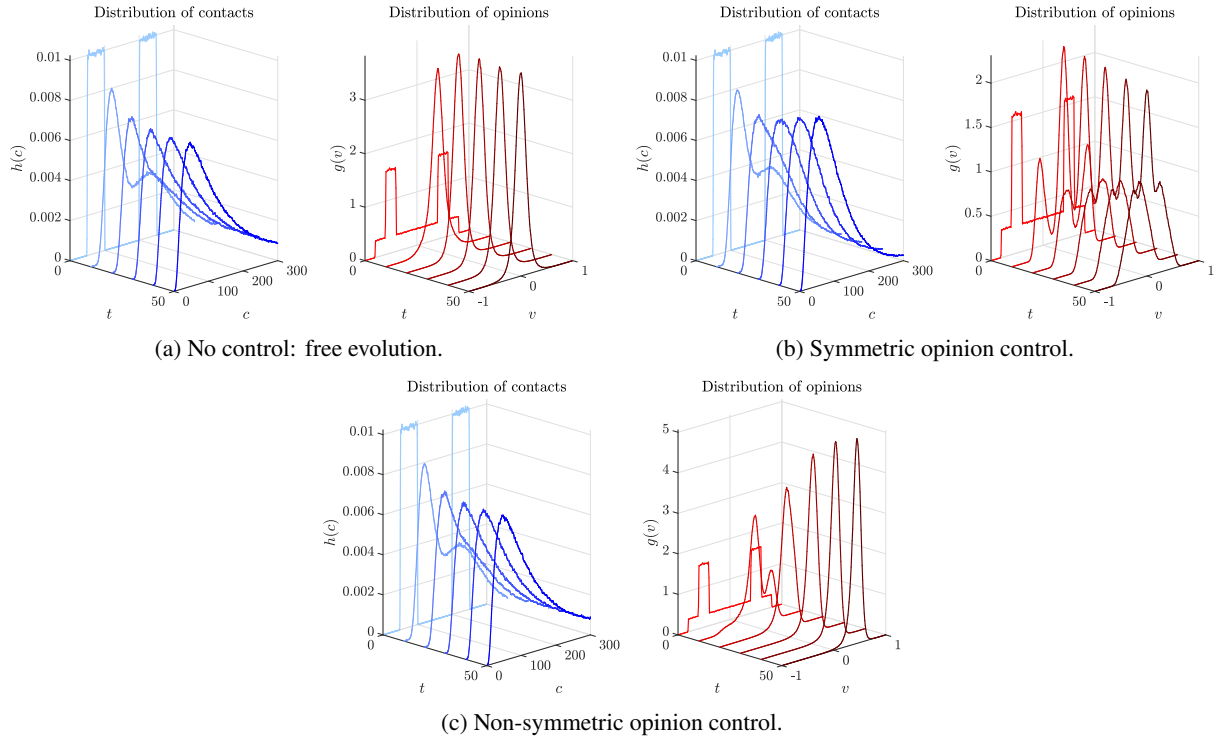


Figure 8: Test 2. Time evolution of the marginal distributions of contacts and opinions at different times. Each panel shows both distributions together: contacts (left) and opinions (right), (a) uncontrolled dynamics; (b) symmetric opinion control; (c) non-symmetric opinion control.

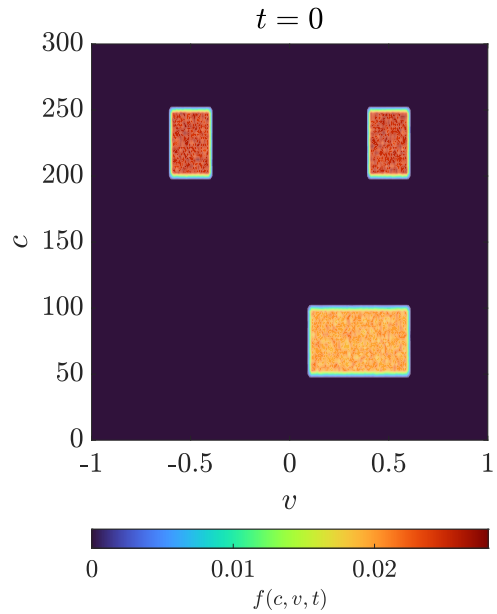


Figure 9: Test 3. Joint density $f(c, v, 0)$ at the initial time.

indirectly, the weakened Group B, whose loss of contacts reduces its influence. In the third scenario, where both leader groups activate the contact control, two persistent and well-connected leader clusters form around their respective target opinions, preventing their decay. In this case, a portion of the follower population converges towards an intermediate compromise opinion, remaining influenced by the simultaneous presence of the two stable leader communities: in other words, a fraction is pulled toward each pole, producing a stable bi-polarization or two echo chambers with a residual central compromise group.

This test highlights the emergence of echo chambers when leader groups preserve their visibility. Leaders who fail to maintain connectivity lose influence, while sustained visibility by one or both groups leads respectively to dominance or to the formation of two stable, polarized communities separated by a small central cluster.

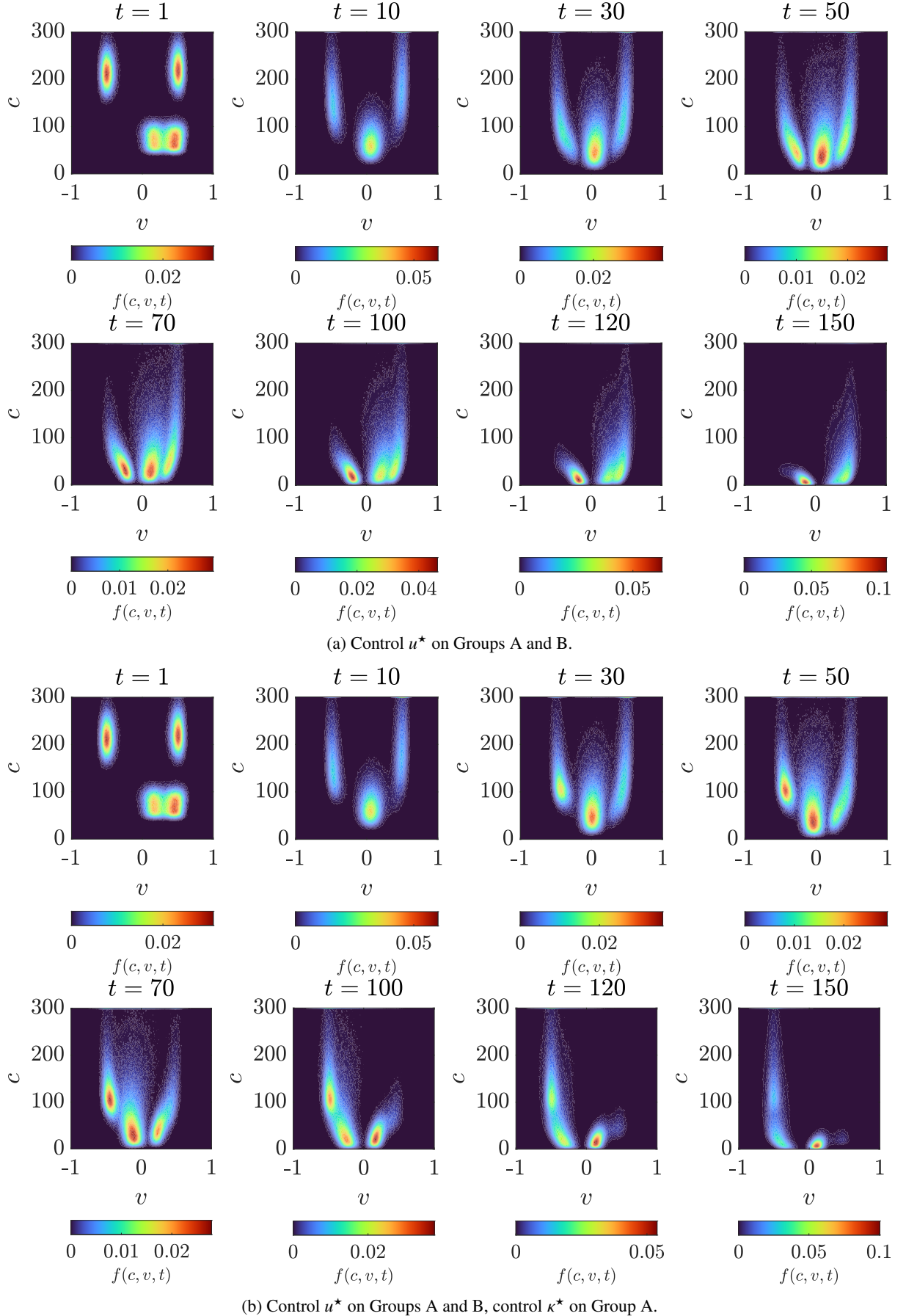
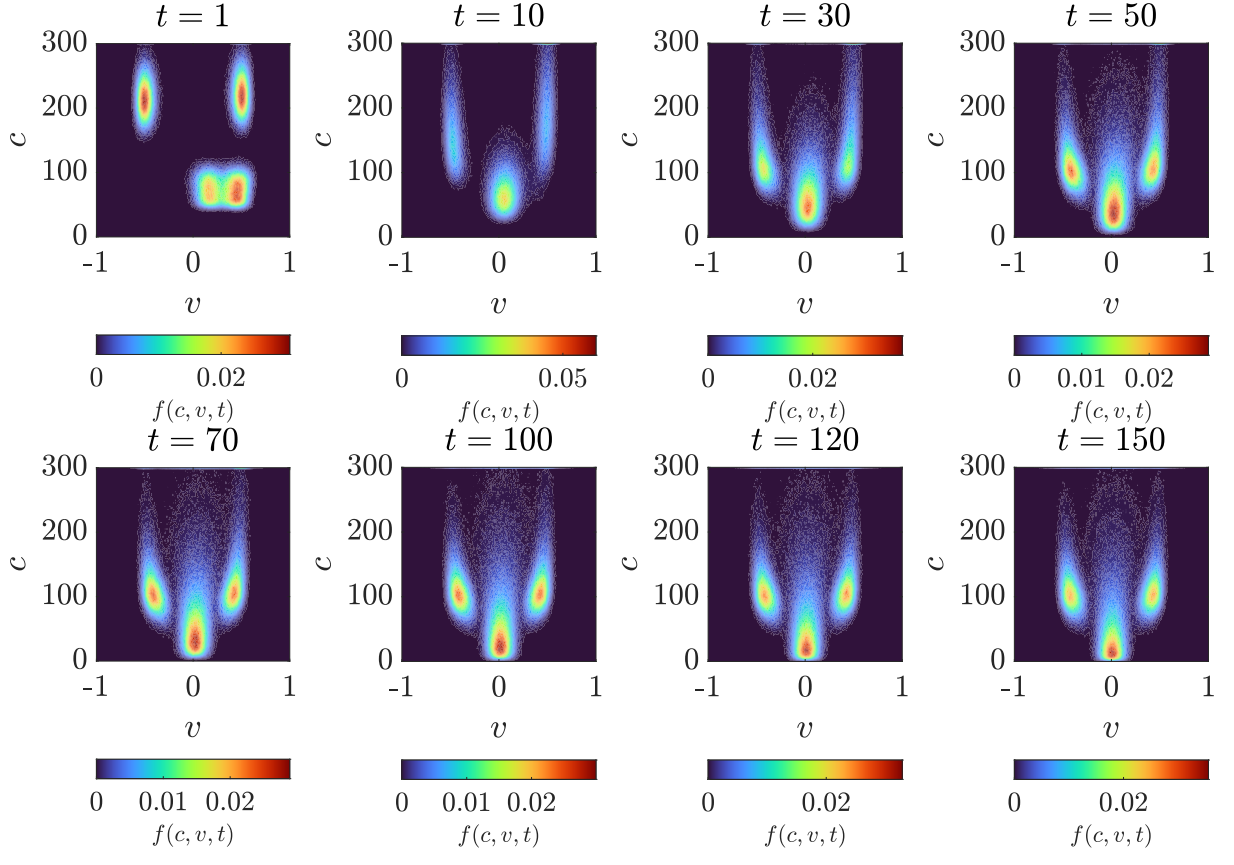


Figure 10: Test 3. Time evolution of the joint density $f(c, v, t)$ in the (v, c) plane. (a) control u^* on Groups A and B.; (b) control u^* on Groups A and B, control κ^* on Group A.



(c) Controls u^* and κ^* on Groups A and B.

Figure 10: (c) controls u^* and κ^* on Groups A and B.

5 Conclusions

In this paper, we have introduced a kinetic modeling framework for opinion dynamics in popularity-adaptive social networks, in which the evolution of opinions is explicitly coupled with the formation and adaptation of social connections. A central feature of the proposed approach is the presence of a feedback mechanism where agents' opinions influence the dynamics of their social contacts, describing the interplay between influence and connectivity. Furthermore, the model include control strategies acting simultaneously on popularity dynamics and opinion exchanges. We believe that such modelling framework allows to reproduce salient features of online social systems, including visibility effects, leader-follower interactions, and opinion-driven reorganization of network connections. Possible extensions of the present work include data-driven calibration and validation of the model using empirical social network data, and the formulation of strategic, game-theoretic settings involving multiple competing controllers with conflicting influence objectives.

Acknowledgments

This work has been written within the activities of GNCS groups of INdAM (Italian National Institute of High Mathematics). GA and MP have been partially supported by MUR-PRIN Project 2022 No. 2022N9BM3N "Efficient numerical schemes and optimal control methods for time-dependent partial differential equations" financed by the European Union Next Generation EU. GA, EC, and MP have been partially supported by MUR-PRIN 2022 through the PNRR Project No. P2022JC95T "Data-driven discovery and control of multi-scale interacting artificial agent systems" financed by the European Union Next Generation EU. EC acknowledges the support by Fondo Italiano per la Scienza (FIS2023-01334) advanced grant "ADvanced numerical Approaches for MULTiscale Systems with uncertainties" - ADAMUS.

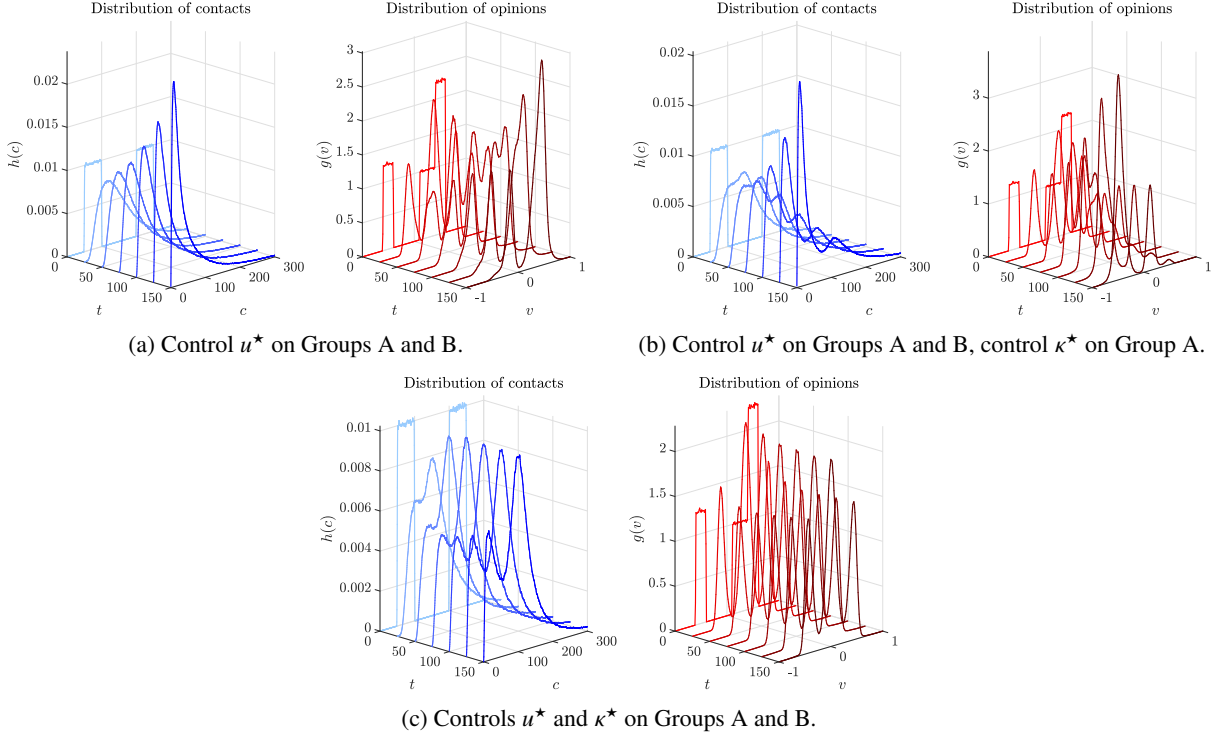


Figure 11: Test 3. Time evolution of the marginal distributions of contacts and opinions at different times. Each panel shows both distributions together: contacts (left) and opinions (right), (a) control u^* on Groups A and B; (b) control u^* on Groups A and B, control κ^* on Group A; (c) controls u^* and κ^* on Groups A and B.

References

- [1] Daron Acemoglu and Asuman Ozdaglar. Opinion dynamics and learning in social networks. *Dynamic Games and Applications*, 1, 2011.
- [2] Giacomo Albi, Nicola Bellomo, Luisa Fermo, Seung Yeal Ha, Jeongho Kim, Lorenzo Pareschi, David Poyato, and Juan Soler. Vehicular traffic, crowds, and swarms: from kinetic theory and multiscale methods to applications and research perspectives. *Math. Models Methods Appl. Sci.*, 29(10):1901–2005, 2019.
- [3] Giacomo Albi, Sara Bicego, Michael Herty, Yuyang Huang, Dante Kalise, and Chiara Segala. Data/moment-driven approaches for fast predictive control of collective dynamics. In *Model Predictive Control: Engineering Methods for Economists*, pages 29–54. Springer, 2025.
- [4] Giacomo Albi, Mattia Bongini, Emiliano Cristiani, and Dante Kalise. Invisible control of self-organizing agents leaving unknown environments. *SIAM Journal on Applied Mathematics*, 76(4):1683–1710, 2016.
- [5] Giacomo Albi, Elisa Calzola, and Giacomo Dimarco. A data-driven kinetic model for opinion dynamics with social network contacts. *European J. Appl. Math.*, 36(2):264–290, 2025.
- [6] Giacomo Albi, Federica Ferrarese, and Chiara Segala. Optimized leaders strategies for crowd evacuation in unknown environments with multiple exits. In *Crowd Dynamics, Volume 3: Modeling and Social Applications in the Time of COVID-19*, pages 97–131. Springer, 2021.
- [7] Giacomo Albi, Michael Herty, Lorenzo Pareschi, et al. Kinetic description of optimal control problems and applications to opinion consensus. *COMMUNICATIONS IN MATHEMATICAL SCIENCES*, 13(6):1407–1429, 2015.
- [8] Giacomo Albi, Lorenzo Pareschi, and Mattia Zanella. Boltzmann-type control of opinion consensus through leaders. *Philos. Trans. R. Soc. Lond. Ser. A Math. Phys. Eng. Sci.*, 372(2028):20140138, 18, 2014.
- [9] Giacomo Albi, Lorenzo Pareschi, and Mattia Zanella. Opinion dynamics over complex networks: Kinetic modelling and numerical methods. *Kinetic & Related Models*, 10(1), 2017.

[10] Nicola Bellomo, Giovanni Dosi, Damián A. Knopoff, and Maria Enrica Virgillito. From particles to firms: on the kinetic theory of climbing up evolutionary landscapes. *Math. Models Methods Appl. Sci.*, 30(7):1441–1460, 2020.

[11] Nicola Bellomo, Livio Gibelli, Annalisa Quaini, and Alessandro Reali. Towards a mathematical theory of behavioral human crowds. *Math. Models Methods Appl. Sci.*, 32(2):321–358, 2022.

[12] Sara Bicego, Dante Kalise, and Grigoris A Pavliotis. Computation and control of unstable steady states for mean field multiagent systems. In *Proceedings A*, volume 481, page 20240476. The Royal Society, 2025.

[13] Walter Boscheri, Giacomo Dimarco, and Lorenzo Pareschi. Modeling and simulating the spatial spread of an epidemic through multiscale kinetic transport equations. *Math. Models Methods Appl. Sci.*, 31(6):1059–1097, 2021.

[14] Martin Burger, Jan-Frederik Pietschmann, and Marie-Therese Wolfram. Data assimilation in price formation. *Inverse Problems*, 36(6), 2020.

[15] Fabio ACC Chalub, Peter A Markowich, Benoît Perthame, and Christian Schmeiser. *Kinetic models for chemotaxis and their drift-diffusion limits*. Springer, 2004.

[16] Arnab Chatterjee and Bikas K Chakrabarti. Kinetic exchange models for income and wealth distributions. *The European Physical Journal B*, 60:135–149, 2007.

[17] Matteo Cinelli, Gianmarco De Francisci Morales, Alessandro Galeazzi, Walter Quattrociocchi, and Michele Starnini. The echo chamber effect on social media. *Proceedings of the national academy of sciences*, 118(9):e2023301118, 2021.

[18] Stephane Cordier, Lorenzo Pareschi, and Giuseppe Toscani. On a kinetic model for a simple market economy. *Journal of Statistical Physics*, 120:253–277, 2005.

[19] Emiliano Cristiani, Benedetto Piccoli, and Andrea Tosin. *Multiscale modeling of pedestrian dynamics*, volume 12. Springer, 2014.

[20] Giacomo Dimarco, Benoît Perthame, Giuseppe Toscani, and Mattia Zanella. Kinetic models for epidemic dynamics with social heterogeneity. *Journal of Mathematical Biology*, 83(1):4, 2021.

[21] Giacomo Dimarco and Giuseppe Toscani. Kinetic modeling of alcohol consumption. *J. Stat. Phys.*, 177(5):1022–1042, 2019.

[22] Giacomo Dimarco and Giuseppe Toscani. Social climbing and Amoroso distribution. *Mathematical Models and Methods in Applied Sciences*, 30(1):2229–2262, 2020.

[23] Bertram Düring, Jonathan Franceschi, Marie-Therese Wolfram, and Mattia Zanella. Breaking consensus in kinetic opinion formation models on graphons. *Journal of Nonlinear Science*, 34(4):79, 2024.

[24] Bertram Düring, Lorenzo Pareschi, and Giuseppe Toscani. Kinetic models for optimal control of wealth inequalities. *Eur. Phys. J. B*, 91(10):Paper No. 265, 12, 2018.

[25] Simone Fagioli and Gianluca Favre. Opinion formation on evolving network: the dpa method applied to a nonlocal cross-diffusion pde-ode system. *European Journal of Applied Mathematics*, 35(6):748–775, 2024.

[26] Adriano Festa, Andrea Tosin, and Marie-Therese Wolfram. Kinetic description of collision avoidance in pedestrian crowds by sidestepping. *Kinet. Relat. Models*, 11(3):491–520, 2018.

[27] Jonathan Franceschi and Lorenzo Pareschi. Spreading of fake news, competence and learning: kinetic modelling and numerical approximation. *Philos. Trans. Roy. Soc. A*, 380(2224):Paper No. 20210159, 18, 2022.

[28] Serge Galam, Yuval Gefen, and Yonathan Shapir. Sociophysics: A new approach of sociological collective behaviour. i. mean-behaviour description of a strike. *Journal of Mathematical Sociology*, 9(1):1–13, 1982.

[29] Marco Günther, Axel Klar, Thorsten Materne, and Raimund Wegener. An explicitly solvable kinetic model for vehicular traffic and associated macroscopic equations. *Mathematical and computer modelling*, 35(5–6):591–606, 2002.

- [30] Itai Himmelboim, Marc Smith, and Ben Shneiderman. Tweeting apart: Applying network analysis to detect selective exposure clusters in twitter. *Communication methods and measures*, 7(3-4):195–223, 2013.
- [31] Daniel Kahneman and Amos Tversky. Prospect theory: An analysis of decision under risk. In *Handbook of the fundamentals of financial decision making: Part I*, pages 99–127. World Scientific, 2013.
- [32] Miller McPherson, Lynn Smith-Lovin, and James M Cook. Birds of a feather: Homophily in social networks. *Annual review of sociology*, 27(1):415–444, 2001.
- [33] C Thi Nguyen. Echo chambers and epistemic bubbles. *Episteme*, 17(2):141–161, 2020.
- [34] Lorenzo Pareschi and Giuseppe Toscani. *Interacting multiagent systems: kinetic equations and Monte Carlo methods*. OUP Oxford, 2013.
- [35] Lorenzo Pareschi and Giuseppe Toscani. Wealth distribution and collective knowledge: a Boltzmann approach. *Philosophical Transactions of the Royal Society A: Mathematical, Physical and Engineering Sciences*, 372(2028):20130396, 2014.
- [36] Gabriella Puppo, Matteo Semplice, Andrea Tosin, and Giuseppe Toscani. Fundamental diagrams in traffic flow: The case of heterogeneous kinetic models. *Communications in mathematical sciences*, 14:643–669, 2016.
- [37] Walter Quattrociocchi, Guido Caldarelli, and Antonio Scala. Opinion dynamics on interacting networks: media competition and social influence. *Scientific reports*, 4(1):4938, 2014.
- [38] Giuseppe Toscani. Kinetic models of opinion formation. *Communications in mathematical sciences*, 4(3):481–496, 2006.
- [39] Giuseppe Toscani. A multi-agent approach to the impact of epidemic spreading on commercial activities. *Math. Models Methods Appl. Sci.*, 32(10):1931–1948, 2022.